Article

# Strong Solute–Solute Dispersive Interactions in a Protein–Ligand Complex

Richard Malham, Sarah Johnstone, Richard J. Bingham, Elizabeth Barratt, Simon E. V. Phillips, Charles A. Laughton, and Steve W. Homans

*J. Am. Chem. Soc.*, **2005**, 127 (48), 17061-17067• DOI: 10.1021/ja055454g • Publication Date (Web): 11 November 2005



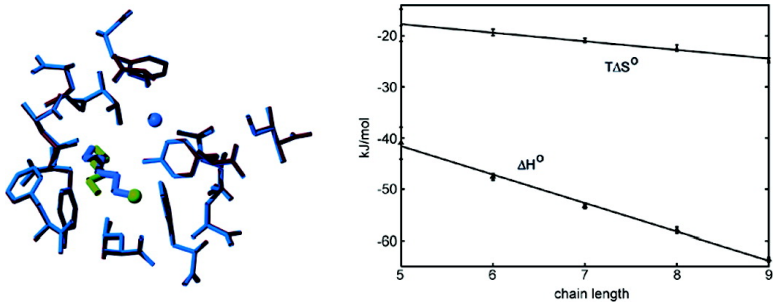


## More About This Article

Additional resources and features associated with this article are available within the HTML version:

- Supporting Information
- Links to the 4 articles that cite this article, as of the time of this article download
- Access to high resolution figures
- Links to articles and content related to this article
- Copyright permission to reproduce figures and/or text from this article

View the Full Text HTML

J|A|C|S
ARTICLES
Published on Web 11/11/2005

# Strong Solute−Solute Dispersive Interactions in a Protein−Ligand Complex

Richard Malham,[†] Sarah Johnstone,[†] Richard J. Bingham,[†] Elizabeth Barratt,[†] Simon E. V. Phillips,[†] Charles A. Laughton,[‡] and Steve W. Homans*,[†]

*Contribution from the Astbury Centre for Structural Molecular Biology, School of Biochemistry & Molecular Biology, University of Leeds, Leeds LS2 9JT, U.K., and Centre for Biomolecular Sciences, School of Pharmacy, University of Nottingham, Nottingham NG7 2RD, U.K.*

Received August 10, 2005; E-mail: s.w.homans@leeds.ac.uk

***Abstract:*** The contributions of solute−solute dispersion interactions to binding thermodynamics have generally been thought to be small, due to the surmised equality between solute−solvent dispersion interactions prior to the interaction versus solute−solute dispersion interactions following the interaction. The thermodynamics of binding of primary alcohols to the major urinary protein (MUP-I) indicate that this general assumption is not justified. The enthalpy of binding becomes more favorable with increasing chain length, whereas the entropy of binding becomes less favorable, both parameters showing a linear dependence. Despite the hydrophobicity of the interacting species, these data show that binding is not dominated by the classical hydrophobic effect, but can be attributed to favorable ligand−protein dispersion interactions.

## Introduction

The hydrophobic effect lies at the heart of many biomolecular recognition processes. The origin of this effect resides in the low solubility of nonpolar compounds in aqueous solution due to the unfavorable decrease in entropy of hydrating waters.[1−3] The association of two nonpolar species in aqueous solution results in the expulsion of ordered hydrating waters into bulk solvent and is a spontaneous process arising from the favorable increase in entropy of the system. However, the thermodynamics of ligand binding to proteins is often dominated by a favorable change in enthalpy, and the characteristic "entropy-driven" thermodynamic signature at physiological temperature is often not observed.[4]

MUP-I is one of a series of variants of the major urinary protein, which is an abundant pheromone-binding protein found in male mouse urine, where subtle recognition of a series of related compounds is essential to its biological function.[5,6] A number of small hydrophobic molecules can bind within the cavity, and the protein is thus an ideal model system with which to study binding thermodynamics of hydrophobic ligands. Recently, we presented evidence that the binding pocket of MUP-I is sub-optimally hydrated.[7] The partial occlusion of the protein binding site from solvent should thus result in an inequality between solvent−solute dispersive interactions that exist prior to the association versus solute−solute dispersive interactions following the association.[8] We suggested that this imbalance might in turn account for the favorable enthalpy of binding of the pheromone 2-isobutyl-3-methoxypyrazine to MUP-I. The serendipitous discovery in our laboratory that MUP-I binds a series of primary aliphatic alcohols, whose solution thermodynamics are well documented,[9] permits a verification of this hypothesis and an experimental estimate of the strength of solute−solute dispersion energies.

## Materials and Methods

**X-ray Crystallography. (i) Crystallization and Data Collection.** Optimal conditions for crystallization of 55 mM CdCl, 100 mM malate buffer pH 4.9, and 18 °C were based on previously identified conditions.[10] Drops containing 2 $\mu$L of MUP-I (10 mg/mL) and 2 $\mu$L of reservoir solution were equilibrated against reservoir solution by vapor diffusion using the hanging drop method. Crystals of space group $P4_32_12$ grew over a period of 5−10 days. Crystal soaks were conducted by the addition of neat alcohol to the reservoir solution to a final concentration of 1% (v/v). This was then allowed to equilibrate with the drop for 6−24 h. Crystals were flash-frozen in liquid nitrogen after soaking for 1 min in a cryoprotecting solution consisting of reservoir solution with the addition of 30% (v/v) glycerol and 1% (v/v) corresponding alcohol. Data collection of pentan-1-ol-, hexan-1-ol-, and heptan-1-ol-soaked crystals was conducted on the laboratory X-ray source, which consisted of a rotating anode generator (RU-H3R, Rigaku), Confocal Max-Flux

[†] University of Leeds.
[‡] University of Nottingham.

(1) Frank, H. S.; Evans, M. W. *J. Chem. Phys.* **1945**, *13*, 507−532.
(2) Nemethy, G.; Scheraga, H. A. *J. Chem. Phys.* **1962**, *36*, 3382−3400.
(3) Tanford, C. H. *The Hydrophobic Effect*; John Wiley and Sons: New York, 1980.
(4) Ross, P. D.; Subramanian, S. *Biochemistry* **1981**, *20*, 3096−3102.
(5) Zídek, L.; Novotny, M. V.; Stone, M. J. *Nature Struct. Biol.* **1999**, *6*, 1118−1121.
(6) Zídek, L.; Stone, M. J.; Lato, S. M.; Pagel, M. D.; Miao, Z. S.; Ellington, A. D.; Novotny, M. V. *Biochemistry* **1999**, *38*, 9850−9861.
(7) Barratt, E.; Bingham, R.; Warner, D. J.; Laughton, C. A.; Phillips, S. E. V.; Homans, S. W. *J. Am. Chem. Soc.* **2005**, *127*, 11827−11834.
(8) Hunter, C. A. *Angew. Chem., Int. Ed.* **2004**, *43*, 5310−5324.
(9) Plyasunov, A. V.; Shock, E. L. *Geochim. Cosmochim. Acta* **2000**, *64*, 439−468.
(10) Bocskei, Z.; Groom, C. R.; Flower, D. R.; Wright, C. E.; Phillips, S. E. V.; Cavaggioni, A.; Findlay, J. B. C.; North, A. C. T. *Nature* **1991**, *360*, 186−188.

***Table 1.*** X-ray Data Collection and Processing Statistics[a]

| | pentan-1-ol | hexan-1-ol | heptan-1-ol | octan-1-ol | nonan-1-ol | decan-1-ol |
|---|---|---|---|---|---|---|
| wavelength (Å) | 1.5418 | 1.5418 | 1.5418 | 1.488 | 0.9795 | 1.488 |
| unit cell | $a = b = 53.5$ | $a = b = 53.2$ | $a = b = 53.6$ | $a = b = 53.7$ | $a = b = 53.5$ | $a = b = 53.7$ |
| dimensions (Å) | $c = 137.0$ | $c = 137.1$ | $c = 137.4$ | $c = 137.6$ | $c = 137.4$ | $c = 137.5$ |
| resolution range (Å) | 1.6−19.5 | 2.0−26.6 | 1.6−19.6 | 2.1−29 | 1.6−42.2 | 1.7−38.0 |
| unique reflections | 26 264 | 13 860 | 26 290 | 12 103 | 27 220 | 23 022 |
| completeness (%) | 96.6 (95.0) | 98.6 (100) | 96.2 (97.1) | 97.4 (93.1) | 99.9 (99.9) | 99.9 (100) |
| multiplicity | 7.1 (7.1) | 5.6 (5.2) | 3.9 (3.5) | 5.9 (5.8) | 6.6 (4.5) | 6.1 (6.7) |
| $R_{sym}$[b] | 0.052(0.27) | 0.094(0.37) | 0.076(0.23) | 0.092(0.13) | 0.092(0.28) | 0.083(0.24) |
| $R_{work}$ | 0.19(0.35) | 0.19 (0.21) | 0.19 (0.35) | 0.19 (0.20 | 0.21 (0.29) | 0.19 (0.20) |
| $R_{free}$ | 0.20 (0.39) | 0.22 (0.25) | 0.22 (0.40) | 0.22 (0.28) | 0.26 (0.38) | 0.23 (0.22) |
| rmsd from ideal: | | | | | | |
| bond length (Å) | 0.011 | 0.013 | 0.011 | 0.012 | 0.012 | 0.012 |
| angles (°) | 1.58 | 1.71 | 1.536 | 1.63 | 1.6 | 1.56 |

[a] Space group for all crystals was $P4_32_12$. [b] Values in parentheses are for the highest resolution shell. $R_{sym} = \sum_{hkl} \sum_i (I_i(hkl) - I_{mean}(hkl))/\sum_{hkl} \sum_i (I_i(hkl))$.

optics (Osmic), and an R-axis IV++ (Rigaku) image plate detector. Data collection of decan-1-ol- and octan-1-ol-soaked crystals was conducted at Daresbury SRS station 14.1. Data collection of nonan-1-ol-soaked crystals was conducted at Daresbury SRS station 14.2. Data were processed and scaled using the programs MOSFLM version 6.10[11] and SCALA.[12]

**(ii) Structure Determination.** The structure of Apo-MUP-I (PDB accession number 1QY0) was used as the phasing model. After several rounds of automatic positional and thermal factor refinement using CNS[13] interspersed with manual remodeling in the program "O",[14] the final statistics shown in Table 1 were produced. Twelve N-terminal residues including the hexa-His tag and eight C-terminal residues were not resolvable due to weak electron density. Crystal coordinates have been deposited in the RCSB protein databank, accession numbers 1ZND, 1ZNE, 1ZNG, 1ZNH, 1ZNK, and 1ZNL.

**ITC Measurements.** ITC experiments on the alcohol series were performed using a MicroCal VP-ITC unit at 300 K. $\Delta C_p$ measurements were made using the same apparatus at three temperatures; 285, 293, 300 K. MUP-I solution was prepared by dialysis of the freeze-dried protein (prepared as detailed[15]) against phosphate-buffered saline (pH 7.4) overnight, followed by subsequent degassing under reduced pressure. The concentration of the protein solution was obtained by measuring UV absorbance ($\epsilon_{280} = 10\,810\ M^{-1}\ cm^{-1}$). The following MUP-I concentrations were used for each experiment: pentan-1-ol, 34.0 $\mu$M; hexan-1-ol (including $\Delta C_p$ measurements), 34.0 $\mu$M; heptan-1-ol, 34.0 $\mu$M; octan-1-ol, 17.0 $\mu$M; and nonan-1-ol, 17.0 $\mu$M. Ligand concentrations were achieved by weighing alcohols (Sigma) and calculating correct amounts for addition to stock (made up with dialysate solvent) using density values provided by the supplier. The following ligand concentrations were used for each experiment: pentan-1-ol, 2.8 mM; hexan-1-ol (including $\Delta C_p$ measurements), 0.75 mM; heptan-1-ol, 0.75mM; octan-1-ol, 0.25 mM; and nonan-1-ol, 0.25 mM. The lower concentrations of octan-1-ol and nonan-1-ol were dictated by the very low solubilities of these alcohols in aqueous buffer solution. ITC experiments comprised an initial ligand injection of 2 $\mu$L followed by 39 injections of 5 $\mu$L with a 240 s interval between each titration. The ITC cell volume was 1.41 mL. The initial data point was deleted from the integrated data to allow for equilibration of ligand/receptor at the needle tip. Heats of dilution for the ligands were determined in control experiments, and these were subtracted from the integrated data before curve fitting. Data were fit in Origin 5.0 (MicroCal) with the standard One Site model based on the Wiseman Isotherm as detailed previously.[15]

**NMR Measurements.** NMR $^1H,^{15}H$ heteronuclear single-quantum correlation (HSQC) spectra were acquired at 500 MHz using a single sample of $^{15}N$-enriched MUP-I at a concentration of 1 mM in 50 mM phosphate buffer, pH 7.0, and a probe temperature of 300 K. Spectra comprised 128 complex data points and 32 transients per $t_1$ increment. Data were processed by zero-filling to 256 complex data points in $t_1$, with cosine-bell squared apodization in both dimensions. Spectra of the apo-protein and in the presence of a 5-fold molar excess of pentan-1-ol, hexan-1-ol, heptan-1-ol, octan-1-ol, and nonan-1-ol were acquired using the same protein solution divided in six equal aliquots.

**Prediction of Binding-Site Water Molecules.** Analysis of potential hydration sites within the binding cavities of each MUP complex was performed using the CMIP methodology.[16] Each crystal structure was stripped of crystallographically determined waters, missing hydrogens were added via the xleap module of Amber8,[17] and partial charges for the alcohols were determined using the RESP procedure[18] from ab initio calculations of molecular electrostatic potentials at the HF/6-31G* level using Gaussian98.[19] The CMIP calculations used an $80 \times 80 \times 80$ grid with a spacing of 0.2 Å centered on the center of mass of the alcohol ligand. To determine which of the predicted water positions were directly associated with the ligand binding cavity, the crystal structures, minus waters, were analyzed using the SurfNet methodology[20] within Chimera.[21] Only CMIP-determined waters that lay within the cavities between the protein and ligand found by SurfNet were retained.

## Results and Discussion

MUP-I binds primary aliphatic alcohols in the series pentan-1-ol through decan-1-ol. We examined the global thermodynamics of binding for pentan-1-ol through nonan-1-ol by use of isothermal titration calorimetry (ITC) measurements[22] at 300 K. The extremely poor solubility of decan-1-ol in aqueous solution prevented reliable measurements for this member of the series. The resulting thermodynamic parameters are shown in Table 2, and typical binding curves are shown in Figure S1 (Supporting Information). Remarkably, the standard enthalpies ($\Delta H_b°$) and entropies ($T\Delta S_b°$) show an approximately linear

(11) Leslie, A. G. W. *CCP4 & ESFEACMB Newsletter On Protein Crystallography*; Daresbury Laboratory: Warington, 1992.
(12) CCP4. *Acta Crystallogr.* **1994**, *D50*, 760−763.
(13) Brünger, A. T.; et al. *Acta Crystallogr.* **1998**, *D54*, 905−921.
(14) Jones, T. A.; Zou, J. Y.; Cowan, S. W.; Kjeldgaard, M. *Acta Crystallogr.* **1991**, *A47*, 110−119.
(15) Bingham, R.; et al. *J. Am. Chem. Soc.* **2004**, *126*, 1675−1681.
(16) Gelpi, J. L.; Kalko, S. G.; Barril, X.; Cirera, J.; de la Cruz, X.; Luque, F. J.; Orozco, M. *Proteins* **2001**, *45*, 428−437.
(17) Case, D. A.; et al. *AMBER 8*; University of California: San Francisco, 2004.
(18) Cieplak, P.; Cornell, W. D.; Bayly, C.; Kollman, P. A. *J. Comput. Chem.* **1995**, *16*, 1357−1377.
(19) Frisch, M. J.; et al. *Gaussian 98*; Gaussian, Inc.: Pittsburgh, PA, 1998.
(20) Laskowski, R. A. *J. Mol. Graph.* **1995**, *13*, 323.
(21) Pettersen, E. F.; Goddard, T. D.; Huang, C. C.; Couch, G. S.; Greenblatt, D. M.; Meng, E. C.; Ferrin, T. E. *J. Comput. Chem.* **2004**, *25*, 1605−1612.
(22) Wiseman, T.; Williston, S.; Brandts, J. F.; Lin, L. N. *Anal. Biochem.* **1989**, *179*, 131−137.

***Table 2.*** Thermodynamic Parameters for the Binding of Primary Alcohols to MUP-I at 300 K Derived from ITC Experiments

| ligand | *n* | $\Delta G_b^\circ$, kJ/mol | $\Delta H_b^\circ$, kJ/mol | $T\Delta S_b^\circ$, kJ/mol | $[\Delta G^\circ_{i2}-\Delta G^\circ_{i1}]$,[b] kJ/mol | | $[\Delta H^\circ_{i2}-\Delta H^\circ_{i1}]$,[b] kJ/mol | | $T[\Delta S^\circ_{i2}-\Delta S^\circ_{i1}]$,[b] kJ/mol | |
|---|---|---|---|---|---|---|---|---|---|---|
| pentan-1-ol | 1.1 | $-23.1 \pm 0.08$[a] | $-41.0 \pm 3.2$ | $-17.9 \pm 3.2$ | $-4.5 \pm 0.1$ | | $-9.7 \pm 3.2$ | | $-5.3 \pm 3.2$ | |
| hexan-1-ol | 0.97 | $-28.3 \pm 0.07$ | $-47.6 \pm 0.6$ | $-19.3 \pm 0.6$ | | $-3.7 \pm 0.1$ | | $-9.1 \pm 0.8$ | | $-5.3 \pm 0.6$ |
| heptan-1-ol | 1.05 | $-32.5 \pm 0.04$ | $-53.4 \pm 0.4$ | $-20.9 \pm 0.4$ | $-2.4 \pm 0.1$ | | $-7.6 \pm 0.7$ | | $-5.2 \pm 0.7$ | |
| octan-1-ol | 1.05 | $-35.6 \pm 0.1$ | $-58.0 \pm 0.6$ | $-22.4 \pm 0.6$ | | $-2.8 \pm 0.2$ | | $-8.9 \pm 0.7$ | | $-6.1 \pm 0.8$ |
| nonan-1-ol | 0.98 | $-38.8 \pm 0.2$ | $-63.6 \pm 0.4$ | $-24.8 \pm 0.5$ | | | | | | |

[a] Errors are derived from duplicate measurements. [b] Values calculated for adjacent "pairs" of ligands using eq 3 and published solvation thermodynamic data for the primary alcohols[9] as follows (all values in kJ/mol): pentan-1-ol, $\Delta G_s^\circ = -11.1$, $\Delta H_s^\circ = -65.0$, $T\Delta S_s^\circ = -53.9$; hexan-1-ol, $\Delta G_s^\circ = -10.4$, $\Delta H_s^\circ = -68.1$, $T\Delta S_s^\circ = -57.7$; heptan-1-ol, $\Delta G_s^\circ = -9.9$, $\Delta H_s^\circ = -71.4$, $T\Delta S_s^\circ = -61.5$; octan-1-ol, $\Delta G_s^\circ = -9.2$, $\Delta H_s^\circ = -74.4$, $T\Delta S_s^\circ = -65.2$. Data for nonan-1-ol were extrapolated from these data to give $\Delta G_s^\circ \approx -8.8$, $\Delta H_s^\circ \approx -77.6$, $T\Delta S_s^\circ \approx -68.8$.

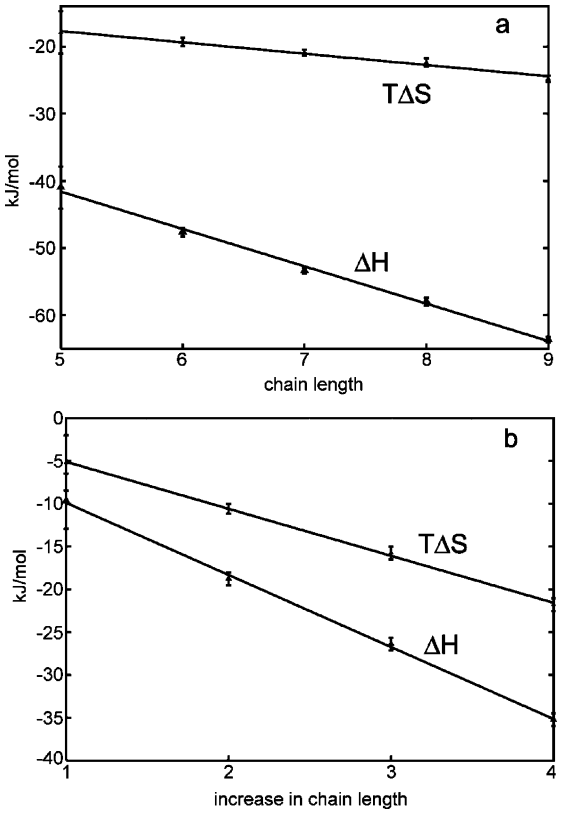


***Figure 1.*** Thermodynamics of binding of primary aliphatic alcohols to MUP-I. (a) Global enthalpies of binding ($\Delta H^\circ_b$) and entropies of binding ($T\Delta S^\circ_b$) plotted versus carbon chain length. (b) Differences between "intrinsic" enthalpies of binding ($[\Delta H^\circ_{i2} - \Delta H^\circ_{i1}]$) and entropies of binding ($T[\Delta S^\circ_{i2} - \Delta S^\circ_{i1}]$) plotted versus increase in chain length.

dependence with respect to carbon chain length (Figure 1a). Moreover, $\Delta H_b^\circ$ becomes more favorable with increasing chain length and $T\Delta S_b^\circ$ becomes less favorable, in contrast to an increasingly favorable entropic contribution that would be anticipated as the ligand becomes more hydrophobic.[23]

To enable a structure-based interpretation of these parameters, the crystal structures of MUP-I in complex with pentan-1-ol through nonan-1-ol were solved, and details of the binding site in each case are shown in Figure 2. The protein structure is essentially unchanged in each complex, and with the exception of heptan-1-ol, a single ordered water molecule is present within the binding pocket. The single water molecules in the pentan-1-ol, octan-1-ol, and nonan-1-ol complexes, and in a similar position in the heptan-1-ol complex, all have similar low *B*-factors (11−13), indicating a very well ordered site, comparable to the main chain of the protein backbone. In contrast, the single water in the hexan-1-ol complex is in a different position than in the three mentioned above and has a higher *B*-factor (40.65); it is therefore more disordered. The two remaining water molecules in the heptan-1-ol complex have high *B*-factors (42.64 and 37.39) and are thus similarly more disordered. The *B*-factors for ligands fall within the range 20−30.

The primary hydroxyl group of each alcohol is hydrogen-bonded to the side-chain hydroxyl group of Tyr 120 either directly (hexan-1-ol and heptan-1-ol) or through a bridging water molecule (pentan-1-ol, octan-1-ol, and nonan-1-ol). Ligand binding falls loosely into two structural classes, with pentan-1-ol and hexan-1-ol binding in a similar orientation and heptan-1-ol, octan-1-ol, and nonan-1-ol binding in an alternative orientation, due to steric hindrance, approximately perpendicular to the first. Pentan-1-ol is also simultaneously observed, with weaker density, in an orientation similar to that of heptan-1-ol, octan-1-ol, and nonan-1-ol (data not shown). However, ITC data indicate a binding stoichiometry of approximately 1 for pentan-1-ol, and the weaker density thus corresponds to a very low affinity binding site that is occupied in the crystal structure by virtue of the high concentration of ligand utilized in the crystal soak (∼100 mM, see Materials and Methods), but this low affinity site is not titrated in ITC experiments where ligand concentration does not exceed ∼300 $\mu$M.

Since the principal thermodynamic parameters are state functions, the binding thermodynamics for a ligand−protein association can conveniently be represented by a conventional Born−Haber cycle[24,25] (Figure 3).

The observed standard free energy of binding for a given ligand L1 ($\Delta G^\circ_{obs1}$ in the cycle represented by dashed lines in Figure 3) is given by

$$\Delta G^\circ_{obs1} = \Delta G^\circ_{i1} + [\Delta G^\circ_{sb1} - \Delta G^\circ_{su1}] \qquad (1)$$

Analogous equations can be written for the standard enthalpy and entropy of binding. It can be seen that the determination of the "intrinsic" standard free energy of binding $\Delta G^\circ_{i1}$ (i.e., in the absence of solvation effects) of a given ligand requires knowledge of $\Delta G^\circ_{obs1}$, together with the solvation free energies of the species before and after association ($\Delta G^\circ_{su1}$ and $\Delta G^\circ_{sb1}$, respectively). In general, these solvation free energies are unknown. However, by focusing on the *differences* between the thermodynamics of binding of related ligands L1 and L2 (the latter represented by the cycle with solid lines in Figure 3), we

(23) Baldwin, R. L. *Proc. Natl. Acad. Sci. U.S.A.* **1986**, *83*, 8069−8072.
(24) Chervenak, M. C.; Toone, E. J. *J. Am. Chem. Soc.* **1994**, *116*, 10533−10539.
(25) Daranas, A. H.; Shimizu, H.; Homans, S. W. *J. Am. Chem. Soc.* **2004**, *126*, 11870−11876.

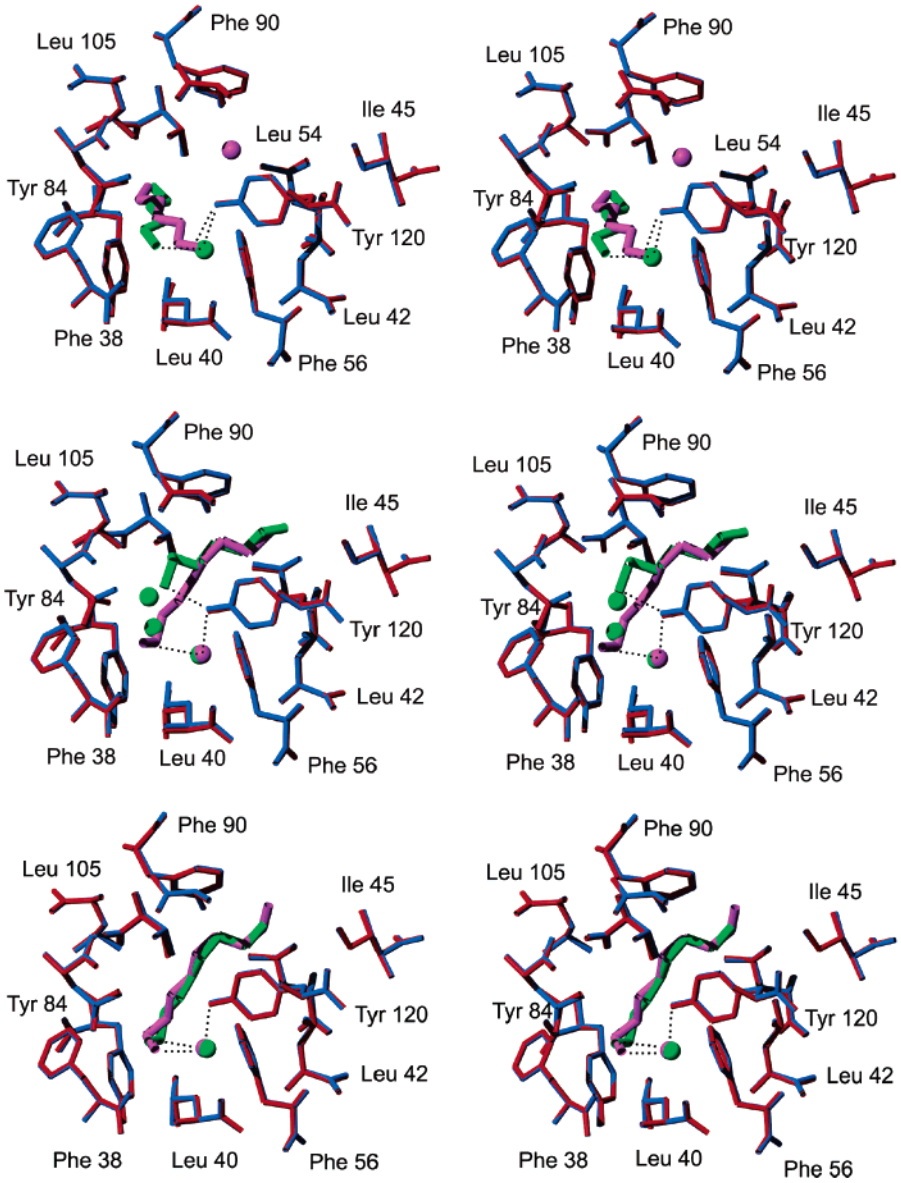


***Figure 2.*** Stereoviews showing details of the binding pocket of MUP-I associated with (top) pentan-1-ol and hexan-1-ol [pentan-1-ol and the associated bound water molecule (sphere) are colored green, whereas hexan-1-ol and the associated water molecule are colored magenta; the protein is colored red in the pentan-1-ol complex and blue in the hexan-1-ol complex], (center) heptan-1-ol and octan-1-ol [heptan-1-ol and the associated bound water molecules are colored green, whereas octan-1-ol and the associated water molecule are colored magenta; the protein is colored red in the heptan-1-ol complex and blue in the octan-1-ol complex], and (bottom) octan-1-ol and nonan-1-ol [octan-1-ol and the associated bound water molecule are colored green, whereas nonan-1-ol and the associated water molecule are colored magenta; the protein is colored red in the octan-1-ol complex and blue in the nonan-1-ol complex]. Dotted lines represent hydrogen bonds from the primary hydroxyl group of each alcohol either directly (hexan-1-ol and heptan-1-ol) or through a bridging water molecule (pentan-1-ol, octan-1-ol, and nonan-1-ol) to the side-chain hydroxyl group of Tyr 120. Crystal coordinates have been deposited in the RCSB protein databank, accession numbers 1ZND, 1ZNE, 1ZNG, 1ZNH, and 1ZNK.

arrive at the following:

$$\Delta G^\circ_{obs2} - \Delta G^\circ_{obs1} = [\Delta G^\circ_{i2} - \Delta G^\circ_{i1}] + \{[\Delta G^\circ_{sb2} - \Delta G^\circ_{sb1}] - [\Delta G^\circ_{su2} - \Delta G^\circ_{su1}]\} \quad (2)$$

If the same number of bound water molecules is present in each complex, $[\Delta G^\circ_{sb2} - \Delta G^\circ_{sb1}] \approx 0$ to first order, and the second term in curly braces in eq 2 will be dominated by the difference in solvation free energy of the free ligands, since solvation of the free protein will be identical in each case. Thus,

$$[\Delta G^\circ_{i2} - \Delta G^\circ_{i1}] \approx [\Delta G^\circ_{obs2} - \Delta G^\circ_{obs1}] + [\Delta G^\circ_{sL2} - \Delta G^\circ_{sL1}] \quad (3)$$

where $\Delta G^\circ_{sL2}$ and $\Delta G^\circ_{sL1}$ are the solvation free energies of ligands L2 and L1, respectively. Equivalent expressions can be written for the enthalpy and entropy.

Inspection of Figure 2 indicates that the complexes of pentan-1-ol, hexan-1-ol, octan-1-ol, and nonan-1-ol with MUP-I contain the same numbers of ordered water molecules. However, it is possible that additional water molecules are located in the binding site which are insufficiently ordered to be observed by X-ray diffraction. The presence of such water molecules might, in principle, complicate further analysis using eq 3, since the equality $[\Delta G^\circ_{sb2} - \Delta G^\circ_{sb1}] \approx 0$ may not be met. Thus, analysis of potential hydration sites within the binding cavities of each MUP complex, with the exception of pentan-1-ol, was performed using the CMIP methodology.[16] We refrained from

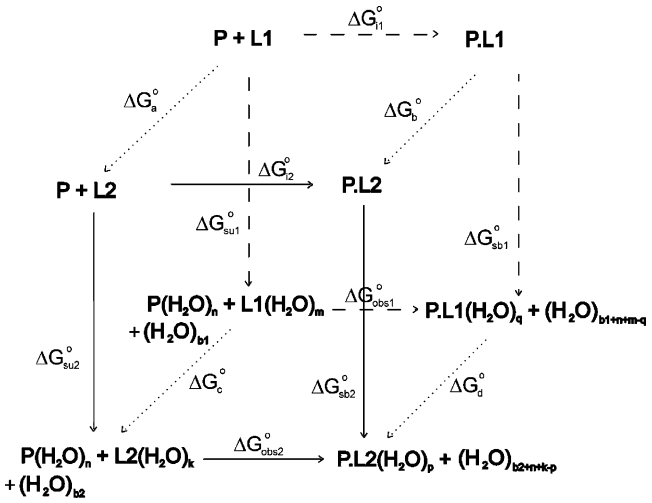


***Figure 3.*** Born−Haber cycle representing the association of two ligands (L1 and L2) with protein P. The standard free energy changes $\Delta G°_a$, $\Delta G°_b$, $\Delta G°_c$, and $\Delta G°_d$ theoretically exist but do not correspond with physically realizable thermodynamic processes.

performing analysis on pentan-1-ol due to the complicating issue of a second ligand molecule in the binding site, as mentioned above. The CMIP titrations, filtered on the basis of the SurfNet analysis[20] (see Materials and Methods), led to the identification of additional water molecules in the binding sites of each complex. From analysis of the distributions, a number of observations can be made. First, there is no consistent trend that increasing size of the alcohol ligand leads to a reduction in the number of water molecules in the binding cavity. Comparing the hexanol and heptanol hydration patterns (Figure 4, upper panel), it can be seen that the displacement of the ligand from one binding site within the cavity to the other is mirrored by the reorganization of the cavity waters. Comparing octanol and nonanol (Figure 4, lower panel), essentially identical predicted hydration patterns can be seen.

Overall, it is clear that the CMIP analysis predicts greater hydration of the MUP complexes than the crystallographic data suggests. However, it must be appreciated that the CMIP procedure calculates only the enthalpic benefit of adding a water molecule to a protein that is otherwise effectively in vacuo, whereas in reality the existence, or not, of such water molecules depends on free energy considerations between entering the binding site or remaining in the surrounding bulk water. CMIP analysis should therefore be regarded as providing an upper limit on hydration. With this in mind, it is particularly significant that we observe no consistent pattern of water displacement with increasing alcohol chain length.

Since the solvation free energies, enthalpies, and entropies of the primary aliphatic alcohols through to octan-1-ol are well documented, [9] it is straightforward to compute differences between the "intrinsic" thermodynamic parameters for two adjacent alcohols in the series according to eq 3, and these values are included in Table 1. In the case of nonan-1-ol, the relevant thermodynamic parameters have not been reported to our knowledge. However, these can readily be approximated by linear extrapolation from members earlier in the series. From the X-ray diffraction data (Figure 2) and the CMIP analysis (Figure 4), we can state with some confidence that the solvation thermodynamics of the complexes of MUP-I with octan-1-ol and nonan-1-ol are essentially identical, and thus the equality $[\Delta G°_{sb2} - \Delta G°_{sb1}] \approx 0$ holds. Remarkably, the relevant "intrinsic" enthalpy and entropy values for these complexes, taken together with those of pentan-1-ol, hexan-1-ol, and heptan-1-ol, are linear with respect to the increase in chain length (Figure 1b). This suggests that the interactions responsible for these thermodynamics are additive, despite the presence of

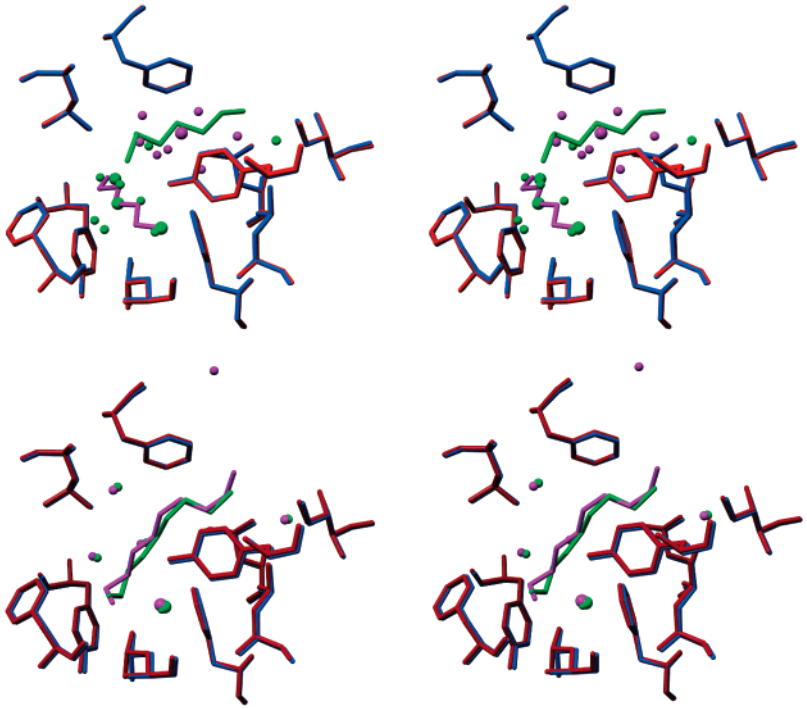

***Figure 4.*** Stereoview of CMIP analysis[16] of MUP-I−alcohol complexes. (Top) Superimposition of the complexes of hexan-1-ol (magenta) and heptanol-1-ol (green); (bottom) superimposition of the complexes of octan-1-ol (magenta) and nonan-1-ol (green). Large spheres in the respective colors show the locations of ordered waters observed by X-ray diffraction (also shown in Figure 2), whereas the smaller spheres show the possible locations of water molecules that are not observed by X-ray diffraction and are thus by implication disordered.

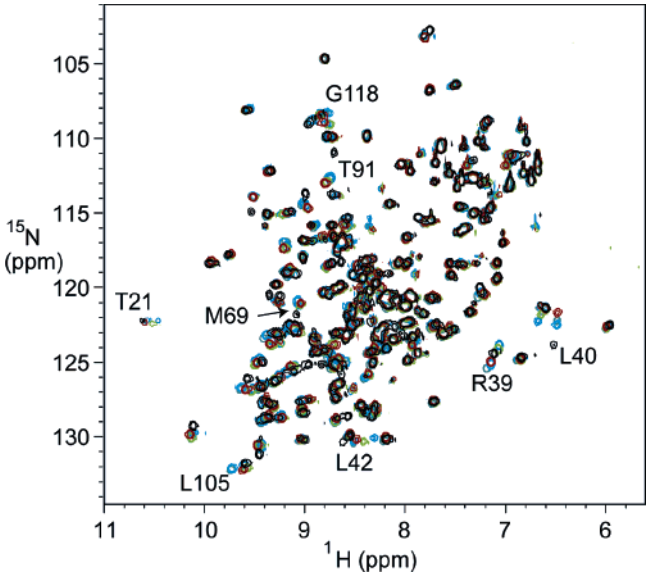


***Figure 5.*** Superimposition of $^{15}$N−$^{1}$H HSQC spectra of MUP-I in the absence of ligand (black contours) and in the presence of a 5-fold molar excess of pentan-1-ol (red contours), hexan-1-ol (green contours), heptan-1-ol (blue contours), octan-1-ol (magenta contours), and nonan-1-ol (gray contours). The vertical scale is the same in each case, and typical residues lining the binding pocket which experience significant shifts are labeled using residue numbering described by Abbate et al.[31]

additional ordered water molecules in the heptan-1-ol complex and the possibility of variable numbers of disordered water molecules throughout the series. The thermodynamic contributions from such water molecules may in any case be quite small—the (enthalpic) hydrogen bond contribution to the stabilization of a buried water molecule in apolar cavities has been reported to be ∼2.5 kJ/mol.[26,27] The entropic contribution from buried water molecules in apolar cavities has not been reported to our knowledge, but will be within the range from 0 to ∼8 kJ/mol.[28]

This linearity of the plots in Figure 1b suggests that there is no cooperativity in the association, in the context defined by Williams and co-workers.[29,30] It follows that the slope of these plots approximates the thermodynamic parameters for the association of a methylene group with MUP-I in the absence of solvation effects. i.e., $\Delta H_{meth}^{\circ} \approx -8.4 \pm 0.2$ kJ/mol and $T\Delta S_{meth}^{\circ} \approx -5.5 \pm 0.1$ kJ/mol. This implies, for example, that the "intrinsic" enthalpic and entropic contributions to binding of, e.g., pentan-1-ol are at least ∼ −40 kJ/mol and ∼ −30 kJ/mol, respectively. In the absence of solvation effects, these contributions must derive either from changes in the structures of the solutes following association or from interactions at the solute−solute interface. X-ray diffraction data (Figure 2) suggest that the structure of MUP-I is essentially unchanged upon binding of any alcohol in the series—the mean global backbone and heavy-atom rmsd's between all four structures are 0.11 ± 0.02 Å and 0.34 ± 0.08 Å, respectively. Moreover, while $^{15}$N and $^{1}$H chemical shift changes are observed in MUP-I upon binding of any member of the series, these changes are restricted to residues within the binding pocket (Figure 5). The exquisite sensitivity of NMR chemical shifts to conformation indicates that minor global structural changes that might not be apparent from the diffraction data do not occur. Each ligand in the bound state clearly adopts a conformation that differs from the minimum energy staggered conformations that exist in free solution. However, deviations from these canonical conformations on binding are enthalpically unfavorable. Thus, the favorable "intrinsic" enthalpic contribution observed must derive from interactions at the solute−solute interface. Given that the empty MUP-I binding pocket is sub-optimally hydrated,[7] it must be anticipated that "intrinsic" binding enthalpy will be dominated by favorable dispersion interactions, arising from the inequality of solvent−solute dispersion interactions before complexation versus solute−solute dispersion interactions after complexation.[8,32] Moreover, the additivity of the intrinsic enthalpy and entropy of binding with respect to chain length suggests that solvent water molecules within the binding pocket serve to offer optimal packing at the solute−solute interface, thus optimizing dispersive interactions.

The origin of the increasingly unfavorable "intrinsic" entropic term progressing through the alcohol series can be understood in large part by the reduction in an additional torsional degree of freedom in the ligand, which has been estimated as ∼6 kJ/mol.[33−36] The value of −5.5 kJ/mol derived here represents an upper limit due to possible contributions from the reduction in degrees of freedom of the protein, as observed previously in MUP-I with a different series of ligands.[15]

Despite the absence of the thermodynamic signature of the "classical" hydrophobic interaction in $\Delta H^{\circ}_{b}$ and $\Delta S^{\circ}_{b}$, evidence[1,37,38] is apparent in the change in heat capacity for the association of, e.g., hexan-1-ol with MUP-I ($\Delta C_p$), which is significantly negative ($-719 \pm 180$ J mol$^{-1}$ K$^{-1}$). Negative $\Delta C_p$ values have been attributed in part to the loss of solvent ordering around hydrophobic species following association.[39] To the extent that ligand binding is a desolvation process, our investigations are not at variance with this hypothesis. However, despite earlier indications to the contrary,[4] the contribution of solute−solute dispersion interactions to binding thermodynamics have not been thought significant, due to the surmised equality between solute−solvent dispersion interactions prior to the interaction versus solute−solute dispersion interactions following the interaction. Our observations indicate that this assumption is not justified. In general, it must be anticipated that the degrees of solvation will vary between proteins bearing hydrophobic binding sites,[26] from sub-optimally hydrated in the case of MUP-I to substantially solvated in, for example, "cleft-like" binding sites such as chymotrypsin.[40] Given the substantial strength of solute−solute dispersive interactions indicated in the current study and from recent theoretical predictions,[41]

(26) Zhang, L.; Hermans, J. *Proteins* **1996**, *24*, 433−438.
(27) Williams, M. A.; Goodfellow, J. M.; Thornton, J. M. *Protein Sci.* **1994**, *3*, 1224−1235.
(28) Dunitz, J. *Science* **1994**, *264*, 670.
(29) Williams, D. H.; Bardsley, B. *Perspect. Drug Discovery Des.* **1999**, *17*, 43−59.
(30) Williams, D. H.; Stephens, E.; O'Brien, D. P.; Zhou, M. *Angew. Chem., Int. Ed.* **2004**, *43*, 6596−6616.
(31) Abbate, F.; Franzoni, L.; Lohr, F.; Lucke, C.; Ferrari, E.; Sorbi, R. T.; Ruterjans, H.; Spinsi, A. *J. Biomol. NMR* **1999**, *15*, 187−188.
(32) Chapman, K. T.; Still, W. C. *J. Am. Chem. Soc.* **1989**, *111*, 3075−3077.
(33) Page, M. I.; Jencks, W. P. *Proc. Natl. Acad. Sci. U.S.A.* **1971**, *68*, 1678.
(34) Searle, M. S.; Williams, D. H. *J. Am. Chem. Soc.* **1992**, *114*, 10690.
(35) Gomez, J.; Freire, E. J. *J. Mol. Biol.* **1995**, *252*, 337.
(36) Lundquist, J. J.; Toone, E. J. *Chem. Rev.* **2002**, *102*, 555−578.
(37) Edsall, J. T. *J. Am. Chem. Soc.* **1935**, *57*, 1506.
(38) Gill, S. J.; Dec, S. F.; Olofsson, G.; Wadsö, I. *J. Phys. Chem.* **1985**, *89*, 3758.
(39) Sturtevant, J. M. *Proc. Natl. Acad. Sci. U.S.A.* **1977**, *74*, 2236−2240.
(40) Talhout, R.; Villa, A.; Mark, A. E.; Engberts, J. *J. Am. Chem. Soc.* **2003**, *125*, 10570−10579.
(41) Vondrasek, J.; Bendova, L.; Klusak, V.; Hobza, P. *J. Am. Chem. Soc.* **2005**, *127*, 2615−2619.

differences in the degree of solvation might offer an explanation for the paradoxical enthalpy driven thermodynamic signature for a substantial number of hydrophobic interactions.

**Acknowledgment.** This work was supported by BBSRC, grant no. 24/B19388 to S.W.H. and grant no. 24/SB11269 to S.E.V.P., and by The Wellcome Trust, grant no. 062164.

**Supporting Information Available:** Complete refs 13, 15, 17, and 19, and a figure illustrating typical ITC binding curves for the association of primary alcohols with MUP-I. This material is available free of charge via the Internet at http://pubs.acs.org.

JA055454G